Available online at www.sciencedirect.com
SCIENCE DIRECT®
ELSEVIER
Ultramicroscopy 102 (2005) 327–337
ultramicroscopy
www.elsevier.com/locate/ultramic

Independent component analysis: A new possibility for analysing series of electron energy loss spectra

Noël Bonnet[a,b,*], Danielle Nuzillard[c]

[a]INSERM, UMRS 514 (IFR53), Hôpital Maison Blanche, 45, rue Cognacq Jay, 51092 Reims Cedex, France
[b]Centre de Recherches en STIC (CReSTIC-LERI), Rue des Crayères, BP 1035, 51687 Reims Cedex 2, France
[c]Centre de Recherches en STIC (CReSTIC-LAM), UFR Sciences Exactes et Naturelles, BP 1039, 51687 Reims Cedex 2, France

Received 11 February 2004; received in revised form 12 November 2004; accepted 22 November 2004

Abstract

A complementary approach is proposed for analysing series of electron energy-loss spectra that can be recorded with the spectrum-line technique, across an interface for instance. This approach, called blind source separation (BSS) or independent component analysis (ICA), complements two existing methods: the spatial difference approach and multivariate statistical analysis. The principle of the technique is presented and illustrations are given through one simulated example and one real example.

PACS: 02.50.Sk; 02.70.−c; 68.35.DV; 82.80.P

Keywords: Electron energy loss spectroscopy; Independent component analysis; Blind separation of sources; Interface; Multivariate statistical analysis

1. Introduction

Improvements in electron energy loss spectroscopy (EELS) techniques have made possible the development of many experimental studies in the field of core-loss spectroscopy, including the study and use of near-edge structures. Among these techniques, the spectrum-image technique (or its spectrum-line variant) plays an important role for performing spatially resolved EELS.

Besides experimental advances, such as the increase of spatial and spectral resolutions, data analysis techniques also play their role in the improvement of the technique. The spatial-difference technique can be cited as one of the data analysis techniques that helped to get useful information from series of spectra recorded across interfaces [1,2]. Another set of methods, dedicated

*Corresponding author. INSERM, UMRS 514 (IFR53), Hôpital Maison Blanche, 45, rue Cognacq Jay, 51092 Reims Cedex, France. Tel.: +33326787771; fax: +33326065861.
E-mail address: noel.bonnet@univ-reims.fr (N. Bonnet).

0304-3991/$ - see front matter © 2004 Elsevier B.V. All rights reserved.
doi:10.1016/j.ultramic.2004.11.003

to larger sets of spectra, comes from multivariate statistical analysis (MSA). [3–5]. The last developments in this category concern the oblique analysis method [6]. These two groups of methods proved already useful but they are also prone to several drawbacks that suggest that more sophisticated methods for analysing series of spectra would be welcome.

In the work described in this paper, we explore a new approach called blind source separation (BSS), or independent component analysis (ICA). This technique has been used to solve many problems in data analysis, signal and image processing. We expect that it could be useful in electron energy-loss spectroscopy, especially when mixtures are involved.

The rest of the paper is organized as follows. In the next section, we briefly summarize the two groups of methods already in use for analysing series of spectra: the spatial difference method and MSA, including oblique analysis. In the following section, we present the general principles of ICA/BSS. Then, we illustrate the application of one of its variants in the field of EELS. Finally, we draw some conclusions and offer some directions for future work.

2. Summary of data analysis methods in use

Here, we concentrate on data analysis methods aiming at discovering unknown spectra within series of recorded spectra. This problem arises for specimens where the EEL spectrum is dominated by the matrix component and an unknown component is present locally at low concentration. The problem may also be to quantify the variation of composition of (known and unknown) components across an interface. Two groups of methods are already in use for trying to cope with these problems.

2.1. The spatial difference approach

This approach deals with two spectra, one of them being recorded in the matrix region and the other being recorded where a variation of the chemical composition is expected. Two variants of the method can be used:

- the difference between the two spectra is computed, after some sort of normalization has been performed on one of the spectra [1]. The resultant difference provides information on the difference between the *new* spectrum and the reference spectrum.
- the spectrum in the region of unknown composition is modelled as a linear combination of the matrix spectrum and the new (unknown) spectrum [2]:

$$S_I = \alpha S_M + (1-\alpha) S_U, \quad (1)$$

where S_I stands for the recorded spectrum, S_M for the matrix spectrum and S_U for the unknown spectrum.

The difficulty is to estimate the coefficient α. This is often done through a trial-and-error approach.

The drawbacks of the spatial difference approach have been identified for a long time: with the first variant, care must be taken to avoid confusing the new spectrum with artefacts due to any energy drift, for instance [7]. With the second variant, the approach remains subjective with respect to the scaling factor, even if general guidelines have been devised for choosing it properly [2,8,9].

A variant of the spatial difference method, called the normalized spatial difference method (NSD) was also suggested by Imhoff et al. [10].

2.2. Multivariate statistical analysis

With the development of the spectrum-line approach [11], or even more with the spectrum-image approach, it becomes worth processing a series of spectra at once rather than pairs of spectra. Multivariate techniques are able to do so and to extract the different sources of information contained in such complete series [3–5]. More specifically, a series of spectra can be decomposed into an average spectrum $\bar{S}$ and a set of orthogonal components Ψ_k common to all the spectra of the series. Any spectrum of the series (S_i) can thus be

represented as a linear combination of the components:

$$S_i = \bar{S} + \sum_{k=1}^{K} \varphi_{ik} \Psi_k \text{ with } \Psi_k \Psi_{k'} = \delta_{kk'}, \quad (2)$$

where δ is the Kronecker symbol, Ψ_k are the components (called eigen-spectra) and φ_{ik} is the weight of component k in spectrum i.

This decomposition (through Principal Components Analysis, Correspondence Analysis, Karhunen–Loeve Analysis, etc.) may be useful for the qualitative interpretation of the data set (number of real components, besides noise, for instance) or for performing a multivariate improvement of the signal-to-noise ratio. However, it does not help very much in the discovery of a *new* chemical component, through its (unknown) spectrum. The main reason for that is that the decomposition performed by MSA is made into *orthogonal* components, also called *abstract* components. Thus, the principal components cannot be identified with the real components, i.e. the spectra of the different elements that enter into the composition of the studied area [5]. One way to go farther is to perform *oblique* analysis after the orthogonal analysis. This means rotating the axes of representation in such a way that they possess a more physical meaning [6]. Although several automatic approaches have been suggested (in other fields of application) for performing the rotation of the axes automatically, the only way we found to perform it with EEL spectra is again through a trial-and-error procedure.[1] This is not completely satisfactory and justifies trying other approaches, such as the one we are investigating in this paper.

3. Blind source separation/independent component analysis

The general problem these methods attempt to solve is that of mixtures of signals, the signals originating from n sources being mixed and recorded by p sensors

$$x_k = \sum_{i=1}^{n} a_{ik} s_i, \quad k = 1 \ldots p. \quad (3)$$

Provided the sources can be considered as statistically independent,[2] solutions can be found to recover them, hence the name *blind source separation* (BSS). These solutions trace back to the work of Jutten and Herault [12]. They often consist of finding an inverse filter that provides outputs as much independent as possible, hence the name *independent component analysis* (ICA).

The different solutions that have been proposed can be summarized as:

- the neuromimetic approach [12]
- several solutions based on the concepts of cumulants and kurtosis

ICA is assumed to be superior to PCA and related methods for non-Gaussian variables. Thus, maximization of the non-Gaussianity may be a strategy for finding independent components. One possible and popular criterion of non-Gaussianity is the kurtosis:

$$\text{kurt}(y) = E\{y^4\} - 3\left(E\{y^2\}\right)^2, \quad (4)$$

where $E\{x\}$ stands for the expected value of the random variable x, or, better, its absolute value.[3]

Another indicator of non-Gaussianity is the negentropy

$$J(y) = H(y_{\text{Gauss}}) - H(y), \quad (5)$$

where y_{Gauss} is the Gaussian random variable with the same covariance as y and $H(y)$ is the differential entropy:

$$H(y) = -\int f(y) \log(f(y)) \mathrm{d}y, \quad (6)$$

$f(y)$ being the probability density function of y.

[1] EEL spectra are more difficult to manage than many other types of spectra because they are not mainly composed of well-separated peaks, even after background subtraction.

[2] While PCA and similar techniques, based on second order statistics, only produce uncorrelated components, ICA is based on higher order statistics and discovers independent components. Independence implies uncorrelatedness but the converse is not true.

[3] Sub-Gaussian random variables possess a negative kurtosis while super-Gaussian variables possess a positive kurtosis.

It has been shown that the negentropy can be approximated by:

$$J(y) \propto \left[E\{G(y)\} - E\{G(y_{\text{Gauss}}\}\right]^2, \quad (7)$$

for practically any non-quadratic function G.[4]

In JADE [13], the statistical independence of the sources is obtained through the joint maximization of the fourth-order cumulants.

In fast-ICA [14], non-Gaussianity is measured by a fixed-point algorithm using an approximation of negentropy through a neural network.

- Infomax [15]: a self-organizing learning algorithm maximizes the information transferred in a network of non-linear units. It constitutes a higher-order generalization of Principal Components Analysis.
- The solution based on the minimum mutual information [16].

The mutual information is a natural measure of the dependence between several variables. It is equivalent to the Kullback–Leibler divergence. Thus, ICA estimation by minimization of mutual information is equivalent to maximizing the sum of the non-Gaussianity of the estimates, as does the maximization of the negentropy.

- The solution based on Renyi's mutual information [17].
- SOBI (Second Order Blind Identification) [18]: the method looks for a unitary matrix which diagonalizes jointly several covariance cross-matrices, thus minimizing the off-diagonal terms. The unitary matrix is parameterised with a complex Given rotation and the criterion is minimized by successive rotations. The algorithm is described with more details in the Appendix.

Our purpose was not to search for the optimal solution in the case of EEL spectroscopy, but to demonstrate that this group of techniques could be a useful alternative to techniques in use at the present time. So, we concentrated on one of the BSS/ICA techniques available: the SOBI algorithm, with which good results were obtained in real space [19,21] and in reciprocal space [20]. In the next section, this algorithm is illustrated in several typical situations.

[4]Note that, for $G(y) = y^4$, the kurtosis criterion is obtained.

4. Illustrations of the proposed approach

4.1. A simple demonstration

First we start with the demonstration that a mixture of unknown EEL spectra can be separated and the pure spectra recovered from the mixture. Fig. 1a displays two spectra, described below.

Fig. 1b shows the results of mixing the two spectra according to the mixture matrix

$$\begin{pmatrix} 0.8 & 0.2 \\ 0.4 & 0.6 \end{pmatrix}.$$

Fig. 1c shows the result of the blind separation of the spectra, using the SOBI algorithm. The recovered mixture matrix was:

$$\begin{pmatrix} 0.78 & 0.22 \\ 0.45 & 0.55 \end{pmatrix}.$$

It can be observed that one spectrum displays negative amplitudes. The result can be improved by applying a positivity constraint. The improved result is displayed in Fig. 1d. The recovered mixture matrix is then:

$$\begin{pmatrix} 0.76 & 0.24 \\ 0.42 & 0.58 \end{pmatrix}.$$

It should be stressed that the result could not be obtained from the raw spectra, but only from the differentiated spectra. The reason for this is that, as stated above, EEL spectra are not composed of separated peaks. As a consequence, raw EEL spectra do not fulfil the conditions for blind separation. They are not even uncorrelated. On the other hand, differentiated spectra fulfil these conditions.[5] Blind separation was thus performed with the differentiated spectra and the resultant

[5]Although sophisticated methods have been developed by one of us [23–25] for performing the robust derivation of EEL spectra, we only used classical band-pass digital filters here. The impulse response of these filters was selected as $h = (-1\ 0\ 0\ 0\ 0\ 0\ 1)$.

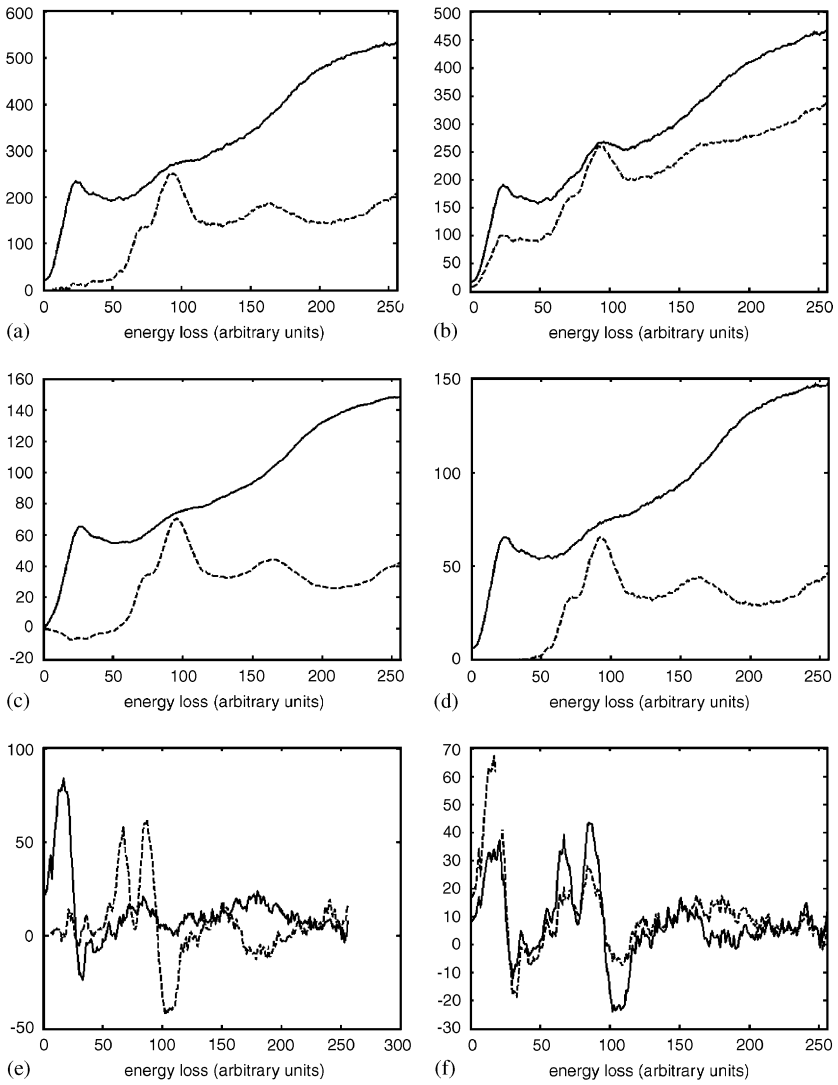

Fig. 1. Illustration of the separation of two-component mixtures: (a) two electron energy-loss spectra, (b) two mixtures of the spectra in (a), (c) recovery of the two spectra, without applying constraints, (d) recovery of the two spectra, with application of a positivity constraint, (e) differentiated original spectra, (f) differentiated mixture spectra.

spectra were then integrated. This is not a problem for subsequent quantification since derivation is a linear process. Differentiated original spectra are displayed in Fig. 1e and the derivatives of the two-component mixture are displayed in Fig. 1f.

4.2. A three-component mixture

Here we consider the problem raised in [22] of a Si–SiO_2 interface where the two spectra far from the interface are known and a third unknown component is suspected close to the interface.[6] The aim of the study is to infer the shape of the unknown spectrum and to deduce the variation of composition across the interface, i.e., the weights of the different spectra in the mixture.

[6]Multivariate Statistical Analysis indicated that three components contributed to the mixtures (see Ref. [6]).

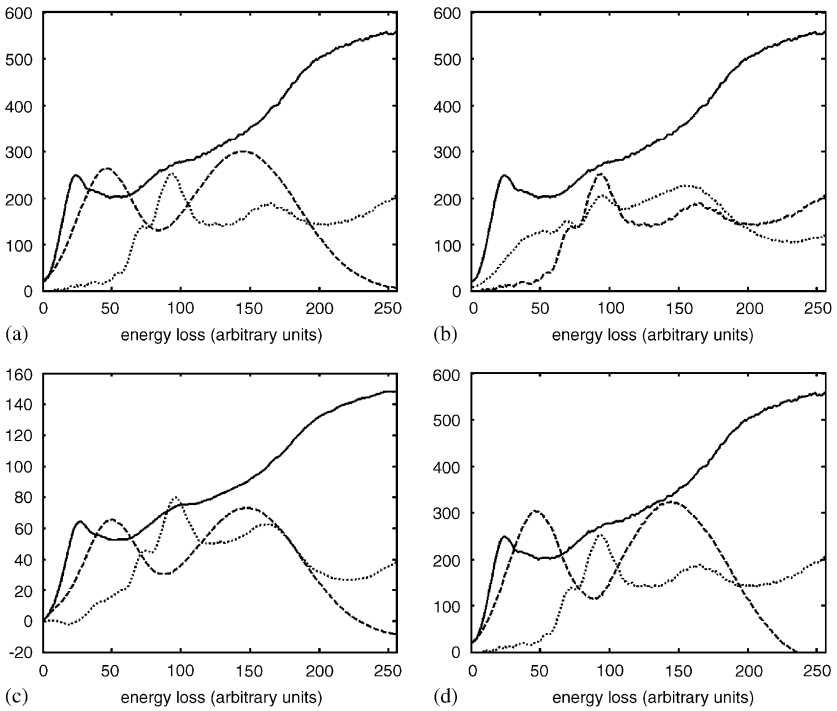

Fig. 2. Illustration of recovering an unknown spectrum from three mixtures with two known spectra: (a) the three spectra: two known and one unknown (two Gaussian bumps), (b) three mixtures of the three spectra, (c) recovery of the three spectra, without constraints, (d) recovery of the three spectra, with the positivity constraint.

As in [6], we start with a simulation of the problem, inserting a hypothetical spectrum as the third component, in order to check to what extent we are able to cope with the problem. The simulated data set is exactly the same as in Ref. [22], so we do not reproduce it here.

Dealing with a three-component mixture and a number of spectra across the interface greater than 3, we have two possibilities. We can process several triplets of spectra, including two pure spectra and one composite spectrum. This will give us several estimations of the unknown component. Alternatively, we can process all the spectra at once. This will give us one global estimation of the unknown spectrum.

Fig. 2 displays the results obtained through the first approach, with two known spectra (the same as in Fig. 1a) and one unknown spectrum, composed of two Gaussian bumps. The mixture matrix used to produce the simulation was

$$\begin{pmatrix} 1.0 & 0.0 & 0.0 \\ 0.57 & 0.43 & 0.0 \\ 0.0 & 0.0 & 1.0 \end{pmatrix}.$$

The mixture matrix found was

$$\begin{pmatrix} 0.90 & 0.0 & 0.10 \\ 0.58 & 0.34 & 0.08 \\ 0.0 & 0.04 & 0.96 \end{pmatrix}.$$

Fig. 2c shows the result obtained without imposing any constraint on the solution. Fig. 2d displays the result obtained when a positivity constraint is imposed on the spectra. The weights of spectra in the mixture are then estimated to be:

$$\begin{pmatrix} 0.93 & 0.0 & 0.07 \\ 0.63 & 0.31 & 0.06 \\ 0 & 0.04 & 0.96 \end{pmatrix}.$$

Another improvement consists in considering that the two extreme spectra, sufficiently far from the interface, are known. The solution obtained with this additional constraint is:

$$\begin{pmatrix} 1 & 0 & 0 \\ 0.58 & 0.41 & 0.01 \\ 0 & 0 & 1 \end{pmatrix}.$$

This result is very close to the simulation.

Fig. 3 displays the results obtained through the second approach, where 21 spectra (mixtures) are used to recover the unknown spectrum. The 21 mixtures of spectra, representing what could be recorded as a spectrum-line across an interface, are displayed in Fig. 3a. The three spectra recovered without the positivity constraint are shown in Fig. 3b. The spectra recovered when using the positivity constraint are shown in Fig. 3c. Fig. 3d shows the mixture matrix (i.e., the weights of the three spectra in the mixtures) across the interface. These values are close to the values introduced during the simulation of the mixtures. The results can still be improved if one can be confident on the fact that spectra far from the interface are *pure* spectra. The results obtained when imposing this constraint are displayed in Fig. 3e (three components) and 3f (weights of the components). In this case, the results correspond perfectly to the simulation. We can conclude that this approach, with a higher number of mixture spectra than the number of components in the mixtures, provides better results than the previous approach, with only as many mixture spectra as components.

In order to see whether the technique can handle more difficult situations, with an unknown spectrum with much lower amplitude, we repeated the previous experiment with the same spectra but with a weaker unknown component at the interface (weight: 11% at maximum). The results are displayed in Fig. 4: Fig. 4a displays the simulated mixture spectra, Fig. 4b the three spectrum components estimated by the SOBI algorithm, Fig. 4c the spectrum components obtained after applying the positivity constraint and the "two-known-spectra" constraint. Fig. 4d displays the weights of the three components estimated in the latter case, compared to the weights used for the simulation. Again, the results obtained with this simulated case are very satisfactory.

Finally, we try to process an experimental set of spectra, described in [22]. Fig. 5a displays a series of 13 electron energy-loss spectra recorded across a Si–SiO_2 interface, for an energy loss between 99 and 124 eV (see Fig. 1 in [6]). Fig. 5b is the result of finding the three expected components when using the SOBI algorithm.[7] Fig. 5c shows the spectra estimated when applying the positivity constraint. One can see that the third component is very similar to the Si edge in SiO_2. Fig. 5d displays the weights of these three components across the interface. One can see that the amplitude of this additional component is very weak, which seems to contradict the results obtained through oblique analysis (see Ref. [6]). The origins of this divergence have still to be elucidated. However, the results shown in Fig. 5d confirm that the interface is not abrupt and that both constituents (Si and SiO_2) diffuse into each other. We also tried to apply the "two-known spectra" constraint. The results are provided in Fig. 5e (estimated spectra) and Fig. 5f (estimated weights). As can be seen on Fig. 5e, the estimated unknown spectrum is still close to the Si spectrum in SiO_2. With this additional constraint, the results come close to those obtained through oblique analysis.

5. Conclusion and future work

Throughout this work, we investigated a new method for analysing series of spectra, to complement two existing methods: the spatial difference method and multivariate statistical analysis. This new approach, independent component analysis (also called blind source separation), aims at discovering unknown sources from series of (at least two) mixtures of these sources. The method is known to be very efficient, provided the unknown sources are really *independent*. Clearly, original EEL spectra do not fulfill the condition of

[7] It was shown previously in the framework of orthogonal multivariate statistical analysis, through several indicators, that this data set cannot be described as a linear combination of two components only. Thus, three components are expected.

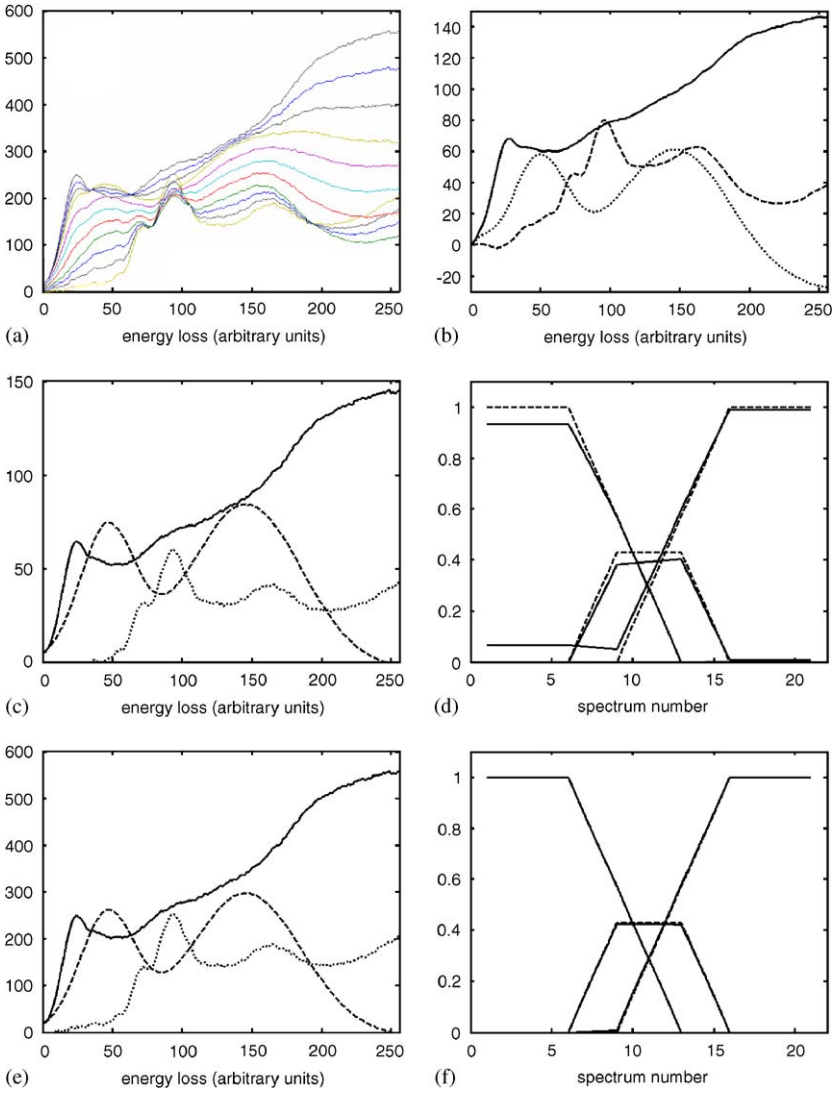

Fig. 3. Illustration of the recovery of one unknown spectrum from a series of mixtures involving three spectra: (a) 21 mixtures, representing a series of spectra across an interface, (b) three recovered spectra, without the application of constraints, (c) three recovered spectra, with the application of the positivity constraint, (d) mixture matrix, i.e., variation of the weight of the three spectra across the interface (the horizontal scale displays the spectrum numbers). The dotted line corresponds to the simulated weights and the plain line corresponds to the estimated weights, (e) three recovered spectra, when spectra far from the interface can be considered as *pure* spectra, (f) the corresponding mixture matrix. Simulated (dotted lines) and estimated (plain lines) values are confused.

independence, since they do not even fulfill the condition of orthogonality. Thus, original (experimental) spectra have to be processed before Independent Component Analysis can be applied. Linear processing is to be preferred, so that quantification can still be performed on the results of the unmixing procedure. Among linear processes, differentiation is one possibility

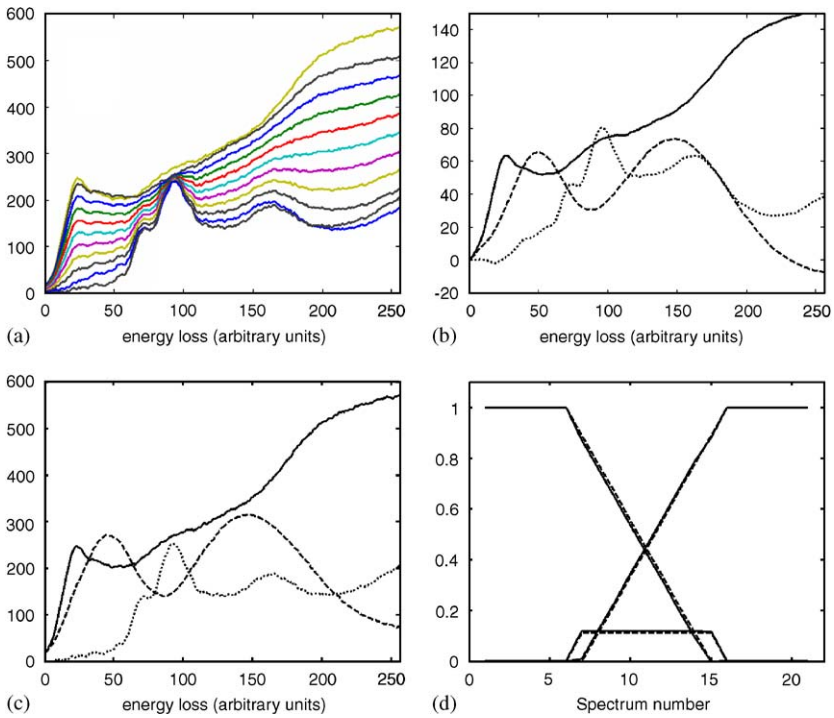

Fig. 4. Illustration of the recovery of one unknown spectrum from a series of mixtures involving three spectra (The unknown spectrum has smaller contributions than in Fig. 3): (a) 21 mixtures, representing a series of spectra across an interface, (b) three recovered spectra, without the application of constraints, (c) three recovered spectra, with the application of the positivity constraint and of the "two-known-spectra" constraint, (d) mixture matrix, i.e., variation of the weight of the three spectra across the interface (the horizontal scale displays the spectrum numbers). Dotted lines: simulated values; plain lines: estimated values.

that we have explored. Empirically, we found that first derivatives produce better results than second derivatives. More theoretical arguments on this topic will be the subject of a further publication.

Thus, we could demonstrate that ICA-BSS can be a good alternative to the spatial difference method and to MSA. We do not claim that this method will systematically outperform previously existing methods but we claim that it may be a useful complementary tool to explore the content of spectrum-lines or spectrum-images.

Compared to the spatial difference approach, the advantages of ICA-BSS are:

- more than two mixture spectra can be handled simultaneously,
- no subjective decision has to be taken by the user.

Compared to the MSA approach and its "oblique" extension, the advantages of ICA-BSS are:

- no "trials and errors" approach has to take place.

The work described here is only an introduction to this new method. More work remains to be done before the technique can be made really efficient:

- the different variants of ICA-BSS must be tried in order to check whether one of them is more appropriate for EEL spectra than the others,

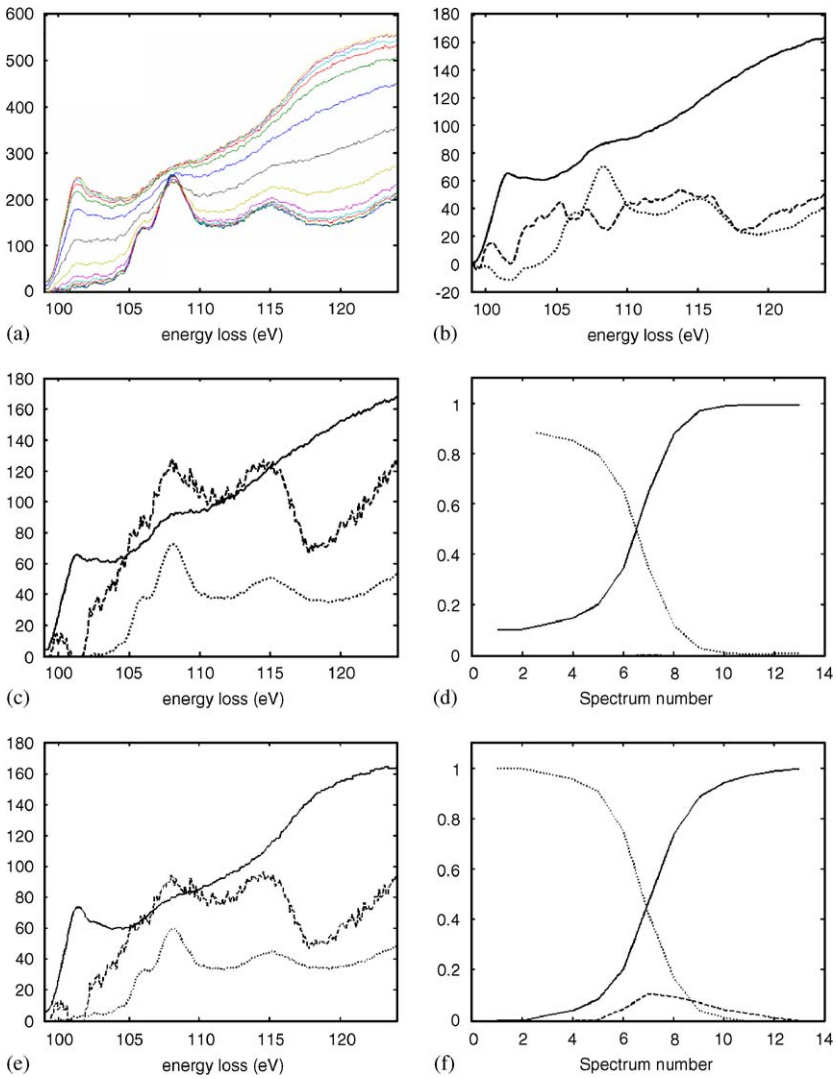

Fig. 5. Illustration of the blind source separation on a real example: (a) thirteen electron energy-loss spectra recorded across a Si–SiO_2 interface (Courtesy of N. Brun, C. Colliex, Laboratoire de Physique des Solides, Orsay), (b) recovered three components by the SOBI algorithm, (c) three spectra recovered with the additional positivity constraint, (d) corresponding weights of the different components across the interface, (e) three spectra recovered with the positivity constaint and the ''two-known spectra'' constraint, (f) corresponding weights of the different components across the interface.

- different variants of spectrum derivatives (first derivative, second derivative, more or less smoothing) have also to be checked,
- the precision and confidence level of the method have to be estimated,
- the sensitivity of the method to noise has also to be studied.

Acknowledgements

The electron energy-loss spectra of the Si–SiO_2 interface were recorded at the electron microscopy unit, Laboratoire de Physique des Solides (CNRS), in Orsay. We thank C. Colliex and N. Brun for allowing us to use them for the illustration of this paper.

We thank the three reviewers of the submitted manuscript for their useful comments that helped to improve this paper significantly.

Appendix

SOBI algorithm

This algorithm was originally proposed by the authors of reference [18] as follows:

1. Estimate the covariance $R(0)$ from T data samples. Calculate the highest eigenvalues $\lambda_1,\lambda_2,\ldots,\lambda_n$ and the corresponding eigenvectors $h_1,h_2,\ldots,h_n$ of $R(0)$.
2. Under the white noise assumption, an estimate σ^2 of the noise variance is the average of the m–n smallest eigenvalues of $R(0)$. The whitened signals, $z(t)=[z_1(t),z_2(t),\ldots,z_n(t)]^T$, are computed as $(\lambda_i-\sigma^2)^{-1/2}\ h_i^* x(t)$ for $1\leqslant i<n$ and the whitening matrix is $W=[(\lambda_i-\sigma^2)^{-1/2}\ h_1,\ldots,(\lambda_n-\sigma^2)^{-1/2}\ h_n]^H$, where H stands for Hermitian.
3. Form sample estimates $R(\tau)$ by computing the sample covariance matrices of $z(t)$ for a fixed set of time lags $\tau\ \varepsilon\ \{\tau_j \mid j=1,\ldots,K\}$.
4. A unitary matrix $\hat{U}$ is then obtained as joint diagonalizer of the set $\{R(\tau_j) \mid j=1,\ldots,K\}$.
5. The source signals are estimated as $\hat{s}(t)=\hat{U}^H.W.x(t)$ and/or the mixing matrix A is estimated as $A=W^{\sharp}.\hat{U}$, where the symbol $\sharp$ is used for conjugate symmetrical.

Note that a unitary matrix is said to be a joint diagonalizer of the set M if it minimizes the criterion C described below, over the set of all unitary matrices. The joint diagonalizer is useful to reduce the probability of an unfortunate choice of time lag τ and to increase the statistical efficiency of the procedure by inferring the value of U from a larger set of statistics.

Consider a set $M=\{M_1,\ \ldots,\ M_k\}$ of K matrices of size $n\times n$. The 'joint diagonality' criterion is defined, for any $n\times n$ matrix V, as the following non-negative function of V: $C(M,V)=\sum_{k=1,K} off(V^H M_k V)$, where in numerical analysis the 'off' of an $n\times n$ matrix M with entries M_{ij} is defined as $\mathrm{off}(M)=\sum_{1\leq i\neq j\leq n}\left|M_{ij}\right|^2$. It means that the unitary diagonalization of a matrix M is equivalent to zeroing off $(V^H M_k V)$ by some unitary matrix V.

A numerically efficient algorithm for performing an exact diagonalization is a generalization of the Jacobi technique of a single hermitian matrix. This technique consists in computing the unitary diagonalizer as a product of Givens rotations.

References

[1] H. Müllejans, J. Bruley, Ultramicroscopy 53 (1994) 351.
[2] H. Müllejans, J. Bruley, J. Microsc. 180 (1995) 12.
[3] N. Bonnet, E. Simova, X. Thomas, Microsc. Microanal. Microstruct. 2 (1991) 129.
[4] N. Bonnet, E. Simova, S. Lebonvallet, H. Kaplan, Ultramicroscopy 40 (1992) 1.
[5] N. Bonnet, Proceedings of the 14th International Congress on Electron Microscopy, Cancun (Mexique). September. 1998, p. 133–134.
[6] N. Bonnet, N. Brun, C. Colliex, Ultramicroscopy 77 (1999) 97.
[7] D.A. Muller, Ultramicroscopy 78 (1999) 163.
[8] H. Gu, M. Ceh, S. Stemmer, H. Müllejans, M. Rühle, Ultramicroscopy 59 (1995) 215.
[9] H. Gu, Ultramicroscopy 76 (1999) 159.
[10] D. Imhoff, S. Laurent, C. Colliex, M. Backhaus-Ricoult, Eur. Phys. J. AP 5 (1999) 9.
[11] C. Colliex, M. Tencé, E. Lefèvre, C. Mory, H. Gu, D. Bouchet, C. Jeanguillaume, Mikrochimica Acta 114/115 (1994) 71.
[12] C. Jutten, J. Hérault, Signal Process. 24 (1991) 1.
[13] J.F. Cardoso, A. Souloumiac, IEE Proc.-F 40 (1993) 362.
[14] A. Hyvärinen, E. Oja, Neural Networks 13 (2000) 411.
[15] A.J. Bell, T.J. Sejnowski, Neural Comp. 7 (1995) 1129.
[16] P. Comon, Signal Proc. 36 (1994) 287.
[17] K.E. Hild, D. Erdogmus, J. Principe, IEEE Signal Process. Lett. 8 (2001) 174.
[18] A. Belouchrani, K. Abed-Meraim, J.-F. Cardoso, E. Moulines, IEEE Trans. Signal Proc. 45 (1997) 434.
[19] D. Nuzillard, A. Bijaoui, Astronomy and Astrophysics, Suppl. Ser. 147 (2000) 129.
[20] D. Nuzillard, S. Bourg, J.-M. Nuzillard, J. Magn. Resonance 133 (1998) 358.
[21] D. Nuzillard, J.-M. Nuzillard, IEEE Signal Proc. Lett. 5 (1998) 209.
[22] N. Brun, C. Colliex, J. Rivory, K. Yu-Zhang, Microsc. Microanal. Microstruct. 7 (1996) 161.
[23] N. Bonnet, J. Michel, D. Wagner, G. Balossier, Ultramicroscopy 41 (1992) 105.
[24] J. Michel, N. Bonnet, D. Wagner, G. Balossier, P. Bonhomme, Ultramicroscopy 48 (1993) 121.
[25] J. Michel, N. Bonnet, Ultramicroscopy 88 (2001) 231.